

# Zonal distribution of sulfotransferase for phenol in olfactory sustentacular cells

Atsushi Miyawaki<sup>1,2</sup>, Hiroshi Homma<sup>3</sup>, Hiro-omi Tamura<sup>3</sup>, Michio Matsui<sup>3</sup> and Katsuhiko Mikoshiba<sup>1</sup>

<sup>1</sup>Department of Molecular Neurobiology, The Institute of Medical Science, The University of Tokyo, 4-6-1 Shirokanedai Minato-ku, Tokyo 108 and <sup>3</sup>Department of Hygienic Chemistry, Kyoritsu College of Pharmacy, 1-5-30 Shibakoen Minato-ku, Tokyo 105, Japan

<sup>2</sup>Present address: Howard Hughes Medical Institute, Cellular and Molecular Medicine, School of Medicine, University of California, San Diego, La Jolla, CA 92093-0647, USA

<sup>2</sup>Corresponding author

**We have immunolocalized phenol sulfotransferase (PST)G, an isoform of PST in sustentacular cells which reside in the dorso-medial portion of the nasal cavity of the mouse. The same topographical pattern of gene expression has been reported for some olfactory neuron-specific genes. When several established (phenol-containing) odorants were used as substrates, mouse nasal tissue cytosol showed a significant level of PST activity, as does mouse liver cytosol. This study is the first to demonstrate that gene expression in the olfactory sustentacular cells is also organized zonally, and indicates the involvement of sulfo-conjugation in olfactory perireceptor processes, such as odorant clearance and xenobiotic detoxification.**

**Keywords:** olfactory epithelium/perireceptor processes/phenol sulfotransferase/sustentacular cells

## Introduction

Sulfotransferases (STs) are phase II drug-metabolizing enzymes that catalyze the coupling of sulfate from 3'-phosphoadenosine-5'-phosphosulfate (PAPS) to molecules possessing phenols, enols, alcohols or amines to form monoesters of sulfuric acid (Mulder and Jakoby, 1990; Falany and Roth, 1993; Matsui and Homma, 1994; Weinshilboum and Otterness, 1994). In liver, for example, conjugation with sulfate confers greater polarity and water solubility on the parent agents, thereby facilitating biliary or urinary excretion and detoxification. Molecular cloning studies have shown that STs belong to a multigene family. Members of this family have significant sequence homologies with one another.

Biotransformation enzymes in the olfactory system are thought to have clearance functions of odorants and detoxification of xenobiotics (olfactory perireceptor processes). The nasal mucosa has a high concentration of phase I (e.g. cytochrome P450; Dahl, 1988) and phase II (e.g. UDP glucuronosyltransferase, glutathione S-transferase) enzymes (Lazard *et al.*, 1991; Ben-Arie *et al.*, 1993). The olfactory epithelium consists of three cell types: sensory neurons, sustentacular or supporting cells,

and basal cells, which are stem cells that generate sensory neurons throughout life. Previous immunohistochemical studies have indicated the presence of two cytochrome P450 isozymes (NMa and NMb) and an olfactory-specific UDP glucuronosyltransferase in sustentacular cells (Lazard *et al.*, 1991; Chen *et al.*, 1992). To examine the involvement of sulfo-conjugation in olfactory perireceptor processes, we investigated the immunolocalization of phenol sulfotransferase (PST) in the mouse nasal tissue. PSTs catalyze the addition of sulfate to a wide variety of phenolic compounds of endogenous and exogenous origin. We used a rabbit antiserum generated against a PST isoform (PSTG) that was purified from rat liver. In male rat livers, all the hepatocytes were immunostained by antiserum to PSTG; in female rat livers, the immunostaining was localized to the hepatocytes proximal to the central vein (pericentral hepatocytes) (Homma *et al.*, 1992).

In our study we immunolocalized PSTG to the cytoplasm of olfactory sustentacular cells. It is likely that sulfo-conjugation works for the clearance or detoxification of inhaled phenolic compounds. In fact, some phenol-containing odorants have been demonstrated to be efficient substrates for the sulfo-conjugating enzymes in the mouse nasal cytosolic fraction.

The identification of a large multigene family encoding odorant receptors (Buck and Axel, 1991) has provided clues to the question of how the olfactory system is organized spatially. Ressler *et al.* (1993) and Vassar *et al.* (1993) have examined the spatial distribution of odorant receptor RNAs in the rodent olfactory epithelium, and have demonstrated that the nasal cavity is divided into different expression zones, which are organized along dorsal-ventral and medial-lateral axes. So far, only sensory neurons in the olfactory epithelium have been shown to be topographically segregated. Here, in contrast, we provide the first evidence of zonal expression in sustentacular cells; those exhibiting PSTG immunoreactivity were found to be localized to the most dorsal and medial zone.

Our observations focus on the following two issues: (i) the involvement of sustentacular cells in the zonal organization of the olfactory epithelium, and (ii) the physiological roles of sulfo-conjugation in olfaction.

## Results

Figure 1A shows a segment of the mouse olfactory epithelium (the upper septum of the posterior nasal cavity) that reacted with the antiserum against PSTG. The immunolabeling was observed throughout the cytoplasm of sustentacular cells. Their oval nuclei, aligned in a single row close to the surface, were clearly outlined. The mucociliary complex at the epithelial surface was intensely stained; the staining appeared to be derived from the sustentacular

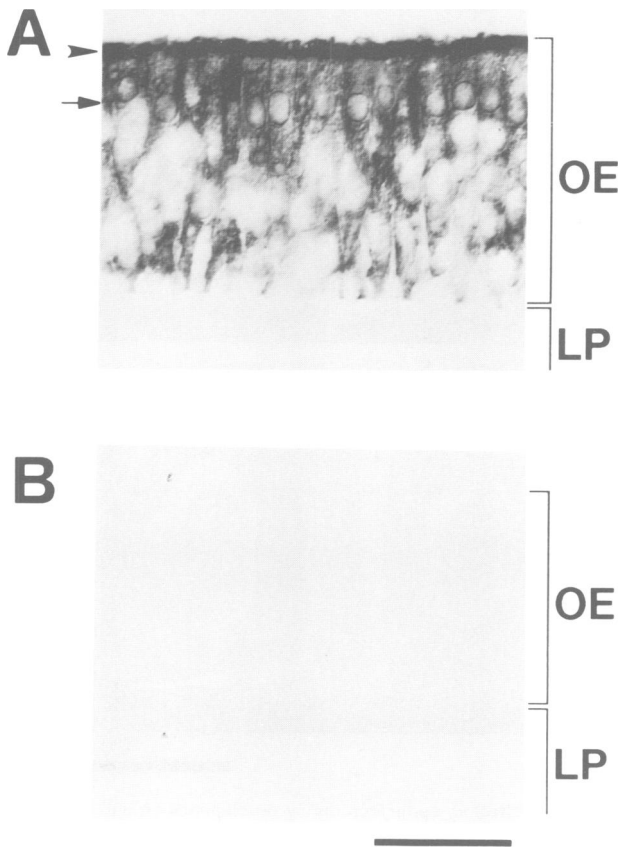


**Fig. 1.** Immunolocalization of PSTG in the olfactory epithelium. Tissue sections (12  $\mu\text{m}$ ) were incubated with an antiserum against PSTG (A) and with a preimmune serum (B). OE, olfactory epithelium; LP, lamina propria. Scale marker, 50  $\mu\text{m}$ .

cell microvilli. Immunoreactivity was not detected in the lamina propria containing Bowman's glands, bundles of olfactory nerve processes and blood vessels. Preimmune serum gave no staining over the nasal mucosa (Figure 1B).

Next we examined the topographical pattern of PSTG expression in the nasal cavity. Figure 2A shows a coronal section of the mouse posterior nasal cavity. PSTG immunoreactivity was symmetrically localized in a dorso-medial region, which covers the roof, the upper septum and the dorsal portions of the endoturbinates (IIa and IIb). A schematic diagram of the coronal section corresponding to Figure 2A is illustrated in Figure 2B. The immunopositive region was identical in different individuals, regardless of gender, and corresponded to the region that hybridized to K18 odorant receptor subfamily probes (Ressler *et al.*, 1993). A similar section was hybridized with a  $^{35}\text{S}$ -labeled probe for the cAMP-gated ion channel gene (Figure 2C). The silver grains, which indicate the presence of olfactory sensory neurons, line most of the nasal cavity. Because sensory neurons and sustentacular cells coexist in every portion of the epithelium, the signal seen in Figure 2C also indicates the distribution of sustentacular cells. Figure 2D shows a section of mouse anterior nasal cavity. PSTG was immunolocalized extensively to the olfactory epithelium lining the roof. No immunoreactivity was observed in the respiratory epithelium or in the vomeronasal organ. Faint signals in the glands of the nasal septum turned out to be nonspecific; they were also detected when reacted with

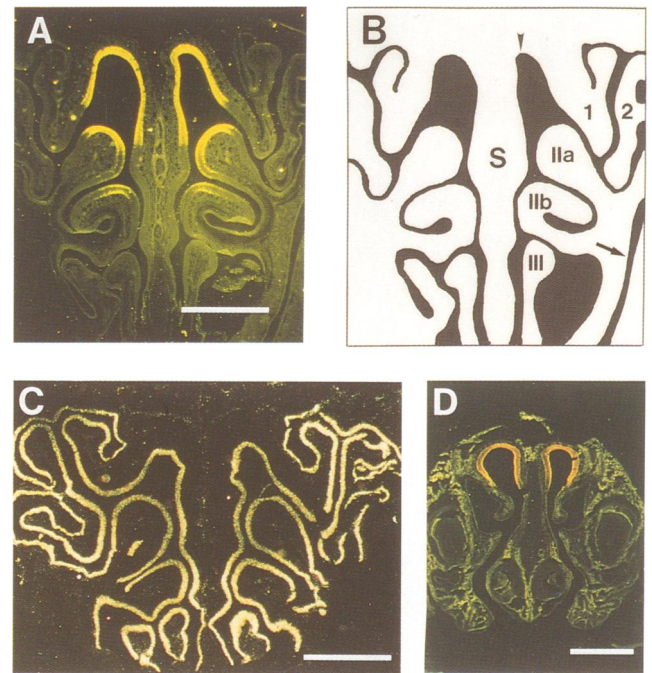


**Fig. 2.** Topographical distribution of PSTG immunoreactivity through the mouse nasal cavity. Low magnification views of posterior (A) and anterior (D) coronal sections. Under dark illumination, DAB precipitates appear as golden spots within the olfactory epithelium. (B) A schematic diagram indicates the locations of the roof (arrowhead), maxillary recess (arrow), septum (S), endoturbinates IIa, IIb and III and ectoturbinates 1 and 2 in (A). (C) To define the extent of the olfactory epithelium, a posterior section was hybridized with a  $^{35}\text{S}$ -labeled cAMP-gated ion channel probe. Scale marker, 1 mm.

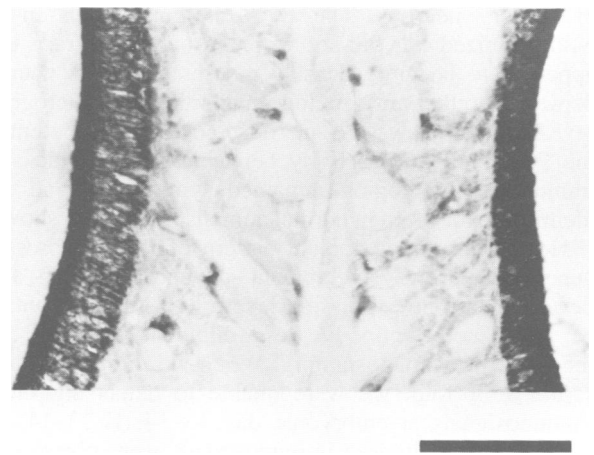


**Fig. 3.** Comparison of immunoreactivity of PSTG in control (left) and neuron-depleted (right) olfactory epithelia of the upper septum. The right olfactory bulb was removed as described in Materials and methods. Scale marker, 1 mm.

preimmune serum. The same immunohistochemical results were obtained using rat nasal cavity (data not shown).

The immunolocalization of PSTG in sustentacular cells was confirmed using unilaterally bulbectomized animals. Destruction of the olfactory bulb causes the retrograde degeneration of sensory neurons in the olfactory epithelium. Figure 3 shows the mouse nasal septum with normal (left) and bulbectomized (right) sides. On the right side, staining for olfactory marker protein (OMP) in the axon bundles was reduced significantly (results not shown), and



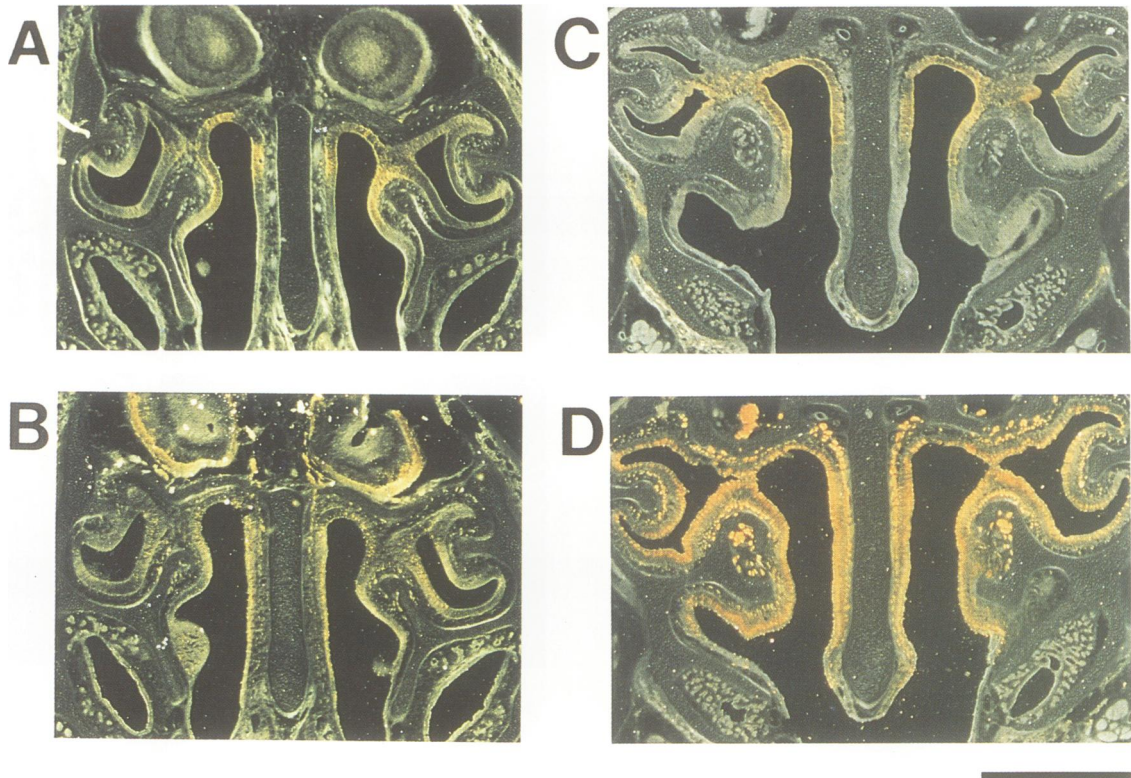


**Fig. 4.** Distribution of immunoreactivity of PSTG (A and C) and OMP (B and D) in the olfactory epithelium during development (A and B, E 15; C and D, P 0). Dark-field photomicrographs were taken as shown in Figure 2A and D. Scale marker, 1 mm.

the epithelium became thin because of the degeneration of sensory neurons. The PSTG immunosignals in the bulbectomized side did not decrease; on the contrary, they appeared to be more densely distributed in the neuron-depleted epithelium. A low magnification micrograph revealed that there was no difference in the extent of the PSTG immunoreactivity between the two sides; the immunopositive region remained symmetrical and was identical to that seen in normal animals (results not shown).

How is the topographical pattern of PSTG expression generated during development in mice? During fetal development, the expression level of PSTG was found to be low; more antibody (less diluted antiserum) was required for immunostaining. When we diluted the antiserum 1350-fold, we were unable to detect significant immunosignals at embryonic day 13–14 (E 13–14). At E 15, the most intense immunosignals were observed in the dorso-medial region of the epithelium, when incubated with 2700-fold diluted antiserum (Figure 4A). Immunohistochemistry for OMP showed that maturing olfactory neurons were distributed more widely (Figure 4B). Along the epithelium of the septum, the boundary of the PSTG immunoreactivity was most evident. However, as a whole, the outline of the immunopositive region was obscure at this stage. At postnatal day 0 (P 0), the PSTG immunoreactivity was well segregated, resulting in the formation of a dorso-medial zone (Figure 4C and D).

We performed an immunoblot analysis using cytosolic fractions from nasal tissue of mouse and rat, and from rat liver. PSTG was originally purified from rat liver. It forms a homodimer with a native molecular mass ( $M_r$ ) of 67 kDa; the subunit  $M_r$  has been determined to be 35 kDa from

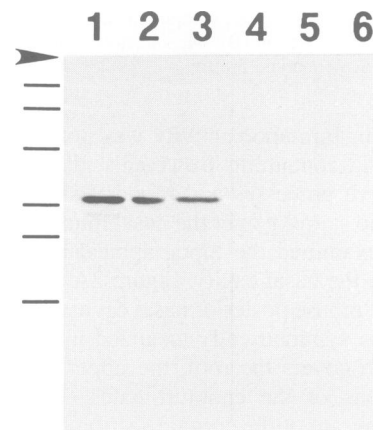


**Fig. 5.** Western blot analysis using antiserum to PSTG. Cytosolic proteins (10  $\mu$ g in each lane) from mouse nasal tissue (lanes 1 and 4), rat liver (lanes 2 and 5) and rat nasal tissue (lanes 3 and 6) were electrophoresed. Antiserum to PSTG (lanes 1–3) and preimmune serum (lanes 4–6) was diluted at 1:10 800. An arrowhead indicates the origin of the gel. Molecular sizes shown on the left are 107, 76, 52, 34, 27 and 19 kDa.

SDS-PAGE (Homma *et al.*, 1991). The 35 kDa PSTG was observed in the rat liver (Figure 5, lane 2) and nasal tissue (Figure 5, lane 3). In the mouse nasal tissue (Figure 5, lane 1), the antiserum detected a major protein band of 35 kDa and a faint band of 32 kDa. Preimmune serum gave rise to no protein band (Figure 5, lanes 4–6).

To assess the functional significance of the mouse olfactory PSTs, we examined their ability to catalyze sulfo-conjugation to a classic PST substrate: 2-naphthol.

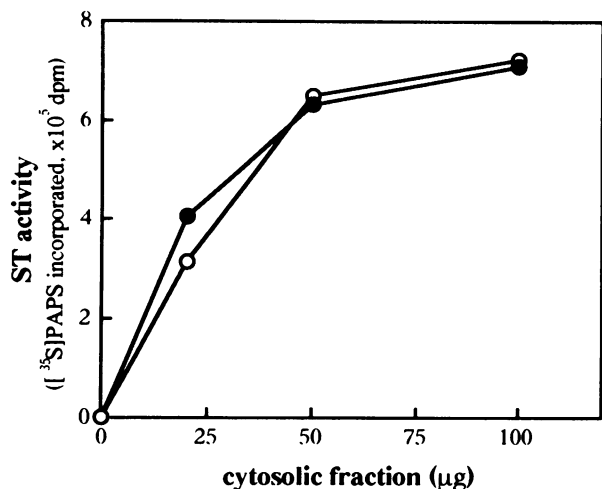


**Fig. 6.** PST activity was measured in the cytosolic fractions of mouse olfactory tissue (closed circles) and liver (open circles). 1  $\mu\text{Ci}$  [ $^{35}\text{S}$ ]PAPS (1  $\mu\text{M}$ ) and 50  $\mu\text{M}$  2-naphthol were used for the assays, as described in Materials and methods. Points represent the averages of duplicate assays. The deviation of each point was  $<5\%$  of the average.

Figure 6 shows the PST activity in the cytosolic fraction of the mouse nasal tissue, which proved to be comparable with that of the mouse liver. Using 10  $\mu\text{g}$  cytosolic fraction, the specific activities of the nasal tissue and liver were determined to be  $0.91 \pm 0.05$  ( $n = 4$ ) and  $0.77 \pm 0.05$  nmol/min/mg ( $n = 4$ ), respectively (Figure 7).

We then studied the sulfo-conjugation activity in the nasal tissue towards 17 different phenol-containing odorants using the assay condition for PST. As shown in Figure 7, of the 17 odorants tested, six (anisyl alcohol, 2,6-diisopropylphenol,  $\alpha$ -methylbenzyl alcohol, prenethyl alcohol, 5-phenyl-1-pentanol and 3-phenyl-1-propanol) were inactive (0.00–0.04 nmol/min/mg), three (cinnamyl alcohol, thymol and 2,6-xyleneol) were moderately reactive (0.19–0.33 nmol/min/mg) and eight (carbacrol, *m*-cresol, eugenol, guaiacol, 4-isopropylphenol, 2-methoxy-4-methylphenol, 2-methoxy-4-propylphenol and vanillyl alcohol) were reactive (0.72–1.40 nmol/min/mg). In general, substrates with a phenolic hydroxyl group were more reactive, while those with an alcoholic hydroxyl group were less reactive. The activity of the liver ST(s) for these odorants was reduced slightly compared with that of the nasal ST(s), with the exception of carbacrol.

## Discussion

### **A zonal organization of gene expression in the olfactory epithelium**

The examination of the spatial distribution of odorant receptor RNAs, which are expressed in the olfactory sensory neurons, has shown that the rodent nasal cavity is divided into different expression zones, being organized along the dorsal–ventral and medial–lateral axes. Our study provides the first evidence of zonal expression in sustentacular cells. We compared the PSTG expression pattern on serial sections along the anterior–posterior axis of the nasal cavity (e.g. Figure 2A and D) with four distinct zones identified in the mouse. The PSTG expression zone is identical to the most dorsal and medial zone, which is designated zone 1 (Ressler *et al.*, 1994). Within

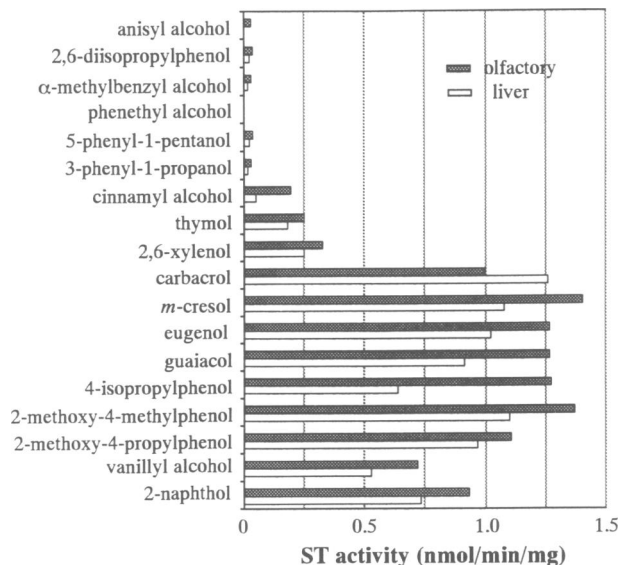


**Fig. 7.** ST activities in the cytosolic fractions of mouse olfactory and liver for various phenol-containing odorants were determined using 0.01  $\mu\text{Ci}$  [ $^{35}\text{S}$ ]PAPS (1  $\mu\text{M}$ ), 50  $\mu\text{M}$  each odorant and 10  $\mu\text{g}$  cytosolic extracts. Hatched and open bars represent the ST activity in the olfactory tissue and liver, respectively. Each bar shows the average value of two assays. The deviations were within 5% of the average values.

zone 1, some subfamilies of odorant receptors are expressed: K18 (Ressler *et al.*, 1993) and M71 (Ressler *et al.*, 1994).

What are the mechanisms for the segregation of gene expression into distinct zones? We would like to discuss this issue in terms of the interaction between olfactory sensory neurons and sustentacular cells (Lewin, 1994).

One possibility is that stem cells for both sensory and sustentacular cells are labeled with zonal identity during the development of the olfactory system. Zonal specification could involve transcription factors that are differentially expressed in different zones. Together with sensory neuron- and sustentacular cell-specific factors, the zonal expression of odorant receptors and PSTG may respectively develop. An intriguing model is that sustentacular cells generate zone-specific molecules which act on sensory neurons during neurogenesis. In this model, primary determination of the zonal pattern occurs in sustentacular cells. Neurogenesis in the olfactory epithelium continues throughout life. Olfactory sensory neurons have a limited life span and are constantly regenerated from basal cells. As sensory neurons differentiate, they migrate apically through the epithelium. Sustentacular cells stretch from the epithelial surface to the basal lamina. Along the extent of the lateral cell membrane, sustentacular cells make contact with basal cells and sensory neurons from all the stages of differentiation. So far little is known about the functional roles of sustentacular cells in neurogenesis.

An alternative possible mechanism for the spatial segregation of gene expression involves the synaptic connections between olfactory sensory neurons and olfactory bulb neurons. Several reports have suggested that the two organs interact in such a way that the development of one may be regulated by the other. Contact with individual glomeruli might bring about functional stimulation, which

governs the expression of some genes in sensory neurons. They include zone-specific genes such as odorant receptor genes. Sensory neurons may then generate signals that control gene expression in sustentacular cells, leading to zonal organization in the cell type. Such activity-dependent spatial segregation may occur during embryogenesis. It is interesting to note that the PSTG antigen first appears at E 14–15, when the first synapses between sensory axons and mitral cell dendrites in olfactory bulb neurons develop (Pinching and Powell, 1971; Hinds and Hinds, 1976). However, in adults it appears that the electrical activity of sensory neurons does not contribute to maintenance of the expression of zone-specific genes in sustentacular cells. Olfactory bulbectomy and subsequent degeneration of the sensory neurons did not affect the PSTG immunoreactivity in zone 1.

The screening of a mouse olfactory cDNA library with the antiserum is underway. Further studies on the transcriptional machinery (*cis* and *trans* elements) for the PSTG gene will provide many pieces of information about the molecular mechanisms of zonal organization in the olfactory epithelium.

### **Sulfo-conjugation in olfactory perireceptor processes**

Sulfation is a phase II drug-metabolizing pathway and is mediated by a cytosolic enzyme family, the STs. These are classified into phenol (aryl) ST, hydroxysteroid (or alcohol) ST, estrogen ST and flavonol ST, according to their substrate specificity. Here, we immunolocalized PSTG, an isoform of PST, in the cytoplasm of olfactory sustentacular cells. Sustentacular cells often contain abundant endoplasmic reticulum (ERs) in their supranuclear cytoplasm. The abundance of this organelle suggests a high level of detoxifying enzyme activity. Previous immunohistochemical studies have indicated the presence of two cytochrome P450 isozymes (NMa and NMb) and an olfactory-specific UDP glucuronosyltransferase in sustentacular cells (Lazard *et al.*, 1991; Chen *et al.*, 1992). Odor molecules are assumed to cross the sustentacular cell membrane freely, owing to their hydrophobic properties. They are hydroxylated by phase I enzymes—the cytochrome P450s. The hydroxylated products are then targeted to phase II enzymes, including STs and UDP glucuronosyltransferases. The final biotransformation products that accumulate in the ER lumen are externalized by a vesicular secretion mechanism.

PSTs constitute a family of isoenzymes with partially overlapping substrate specificities. From rat liver, for example, four PST isoenzymes have been purified (PSTs I–IV; Mulder and Jakoby, 1990). However, the organization of the PST family remains unclear. Recent molecular cloning and biochemical studies have indicated that the PST gene family is large, so there should be more isozymes of PST.

PSTG is a PST isoform purified from rat liver (Homma *et al.*, 1991). PSTG has peculiar enzymatic features. During purification, the enzymatic activity was lost after separation by ion-exchange chromatography but was recovered by the addition of guanidine hydrochloride. It has a pH optimum of 5.5 for simple phenolic substrates—1-naphthol, 2-naphthol and 4-nitrophenol—and a pH optimum of 9.0 for dopamine. PSTG forms a homodimer with a

native  $M_r$  of 67 kDa and a subunit  $M_r$  of 35 kDa. Using the antiserum against PSTG, a 35 kDa protein was detected in the cytosol of rat liver and nasal tissue and in mouse nasal tissue. The 32 kDa protein band detected in mouse nasal tissue represents a PST isozyme similar to 35 kDa PSTG, because the subunit  $M_r$  of the STs characterized so far ranges from 30 to 36 kDa. Obtaining the cDNA clones which encode the 35 and 32 kDa proteins will allow us to establish the molecular identity of PSTG.

Although most of the studies on STs have been performed using liver, enzymatic activities or immunological signals of certain STs have been reported in other tissues, including brain, kidney, lung, intestine and platelets (Mulder and Jakoby, 1990; Falany and Roth, 1993; Matsui and Homma, 1994; Weinshilboum and Otterness, 1994). Here we have demonstrated that mouse nasal tissue has comparable PST activity with mouse liver. Under the assay condition employed here for PST, odorants with a phenolic hydroxyl group were well sulfated. Among them, guaiacol and eugenol were also shown to be efficient substrates for the olfactory UDP glucuronosyltransferase (Lazard *et al.*, 1991). It is likely that sulfo- and glucuronic acid-conjugations work together in the olfactory system as phase II drug-metabolizing reactions. The ST activity profiles of the nasal tissue and liver were similar to each other at pH 6.4.

The most dorso-medial region of the nasal cavity (zone 1) is the primary site that is exposed to the highest concentrations of inhaled chemicals. The presence of PSTG in zone 1 implies that sulfo-conjugation works to protect olfactory sensory cells from phenol-containing toxic compounds. Alternatively, PSTG may be involved in clearing phenolic odorants from the epithelium after the specific reception, and may thus play a role in modulating the activation of the olfactory epithelium for odor discrimination. If this is the case, it is possible that the substrates of PSTG may preferentially activate the olfactory neurons within zone 1.

## **Materials and methods**

### **Immunohistochemistry of PSTG**

Mice or rats (10 weeks old, male or female) were anesthetized with Nembutal and perfused transcardially with ice-cold PBS followed by ice-cold Zamboni's fixative. The dissected tissues were placed in ice-cold fixative for 2 h, and embedded in OCT compound (Miles). Cryostat sections (10–14  $\mu$ m) were treated with 0.3%  $H_2O_2$  in methanol for 30 min, permeabilized with 0.05% Triton X-100 for 5 min, and treated with PBS containing 1% skimmed milk for 1 h. The sections were incubated for 2 h with a primary antiserum diluted 1:10 800 in PBS. For the sections from developing mice, the antiserum was diluted 1:1350 or 1:2700. Control sections were incubated with a preimmune serum. Horseradish peroxidase (HRP)-conjugated donkey anti-rabbit IgG (Amersham) and diaminobenzidine (DAB) were used as the second antibody and chromogen, respectively. Dark-field photomicrographs were taken such that the unstained portions were also visualized.

### **Immunohistochemistry of OMP**

For several of the sections, an antiserum to OMP (generously supplied by Dr Frank Margolis, Roche Institute of Molecular Biology, Nutley, NJ) was used at a dilution of 1:1600 for 2 h. The sections were treated with rabbit anti-goat IgG biotinylated secondary antibody (Zymed) at a 1:8000 dilution and HRP-conjugated avidin (1  $\mu$ g/ml).

### **In situ hybridization**

Based on the sequence of a rat cAMP-gated ion channel (Dhallan *et al.*, 1990), we carried out a RT-PCR and obtained a full-length cDNA clone

of the mouse channel. Hybridization was performed on the cryosections as described previously (Miyawaki *et al.*, 1994) with a <sup>35</sup>S-labeled cRNA probe prepared from the cDNA clone.

#### Preparation of the cytosolic fraction

To eliminate any contaminated blood cells, male mice (ddY, 10 weeks old) or male rats (Wistar, 9 weeks old) were perfused transcardially with PBS. Nasal mucosa and liver were frozen in liquid nitrogen and ground to a powder in a mortar. The powdered tissue was added to 3 vol ice-cold buffer A (10 mM Tris-HCl, pH 7.4, 250 mM sucrose, 3 mM 2-mercaptoethanol, 0.1 mM EDTA). The cytosolic fraction was obtained by differential centrifugation (2000 g for 10 min, 1600 g for 45 min and 10 500 g for 60 min). The sample was frozen quickly in liquid nitrogen and kept at -80°C. Protein concentrations were determined using the method of Bradford and by employing bovine serum albumin as a standard.

#### Immunoblotting

Cytosolic proteins were resolved by 12.5% SDS-PAGE and electroblotted onto a nitrocellulose membrane (Amersham). The membrane was blocked with 1% skimmed milk in PBS containing 0.1% Tween-20 (PBST), and incubated with antiserum or preimmune serum diluted 1:10 800. After the incubation with peroxidase-conjugated secondary antibody, enhanced chemiluminescence detection was performed as described by the manufacturer (Amersham).

#### Measurement of ST activity

The PST activity in the cytosolic fractions was determined using [<sup>35</sup>S]PAPS as the sulfate donor and 2-naphthol as the sulfate acceptor, according to the procedure described by Foldes and Meek (1973) with a slight modification. The reaction mixture (500 µl) consisted of 10 mM phosphate buffer, pH 6.4, 50 µM 2-naphthol, 1.0 µM [<sup>35</sup>S]PAPS (0.01–0.10 µCi) and cytosolic fraction (10–100 µg). The mixture was incubated at 37°C for 15 min and the reaction was stopped by the addition of 0.1 ml of 0.1 M barium acetate. Then the unconverted [<sup>35</sup>S]PAPS was precipitated by the addition of 0.1 ml each of 0.1 M Ba(OH)<sub>2</sub> and 0.1 M ZnSO<sub>4</sub>. The precipitate was removed by centrifugation at 12 000 g for 5 min. This precipitation procedure was repeated once. The supernatant (300 µl) after the second precipitation was transferred to a 3 ml liquid scintillator and counted. Blanks were monitored by omitting the substrate. For the determination of the activity towards various odorants (Sigma Chemical Co. and Aldrich Chemical Co.), each odorant was diluted or dissolved with distilled water to 1.0–2.5 mM and used as a substrate at a concentration of 50 µM.

#### Bulbectomy

Unilateral bulbectomy permitted the comparison of normal and denervated sides. Male mice (9 weeks old) were anesthetized with Numbtal (25 mg/kg, intraperitoneally). An incision was made between the eyes, and a hole was drilled through the right side of the bone. The right side bulb was aspirated with a narrow glass pipette. The hole was packed with Gelform and the skin was closed. The animals were used 15–20 days later.

## Acknowledgements

We thank Drs Naoko Inoh, Yuki Harada, Naomi Morikawa, Maki Yamada, Shigemoto Fujii, Fumio Matsushita, Hiroyuki Yoneshima and Eiichiro Nagata for technical assistance, and Dr F.L. Margolis for supplying antiserum to olfactory marker protein. We are also grateful to Drs R. Vassar, R.R. Reed, R.Y. Tsien and R. Axel for helpful discussions. This work was supported by grants from the Japanese Ministry of Education, Science and Culture, the Brain Science Foundation, and the Tokyo Biochemical Research Foundation.

## References

Ben-Arie, N., Khen, M. and Lancet, D. (1993) Glutathione S-transferases in rat olfactory epithelium: purification, molecular properties and odorant biotransformation. *Biochem. J.*, **292**, 379–384.  
 Buck, L. and Axel, R. (1991) A novel multigene family may encode odorant receptors: a molecular basis for odor recognition. *Cell*, **65**, 175–187.  
 Chen, Y., Getchell, M.L., Ding, X. and Getchell, T.V. (1992) Immunolocalization of two cytochrome P450 isozymes in rat nasal chemosensory tissue. *NeuroReport*, **3**, 749–752.

Dahl, A.R. (1988) The effect of cytochrome P450-dependent metabolism and other enzyme activities on olfaction. In Margolis, F.L. and Getchell, T.V. (eds), *Molecular Neurobiology of the Olfactory System*. Plenum Press, New York, pp. 51–70.  
 Dhallan, R.S., Yau, K.-W., Schrader, K.A. and Reed, R.R. (1990) Primary structure and functional expression of a cyclic nucleotide-activated channel from olfactory neurons. *Nature*, **347**, 184–187.  
 Falany, C.N. and Roth, J.A. (1993) Properties of human cytosolic sulfotransferases involved in drug metabolism. In Jeffery, E.H. (ed.), *Human Drug Metabolism*. CRC Press, Boca Raton, FL, pp. 101–115.  
 Foldes, A. and Meek, J.L. (1973) Rat brain phenolsulfotransferase. Partial purification and some properties. *Biochim. Biophys. Acta*, **327**, 365–374.  
 Hinds, J.W. and Hinds, P.L. (1976) Synaptic formation in the mouse olfactory bulb. II. Morphogenesis. *J. Comp. Neurol.*, **169**, 41–62.  
 Homma, H., Kamakura, M., Nakagome, I. and Matsui, M. (1991) Purification of a rat liver phenol sulphotransferase (P-ST<sub>G</sub>) with the aid of guanidine hydrochloride treatment. *Chem. Pharm. Bull.*, **39**, 3307–3312.  
 Homma, H., Nakagome, I. and Matsui, M. (1992) Differential localization of sulfotransferase isozymes in rat liver. *Biochem. Biophys. Res. Commun.*, **183**, 872–878.  
 Lazard, D., Zupko, K., Poria, Y., Nef, P., Lazarovits, J., Horn, S., Khen, M. and Lancet, D. (1991) Odorant signal termination by olfactory UDP glucuronosyl transferase. *Nature*, **349**, 790–793.  
 Lewin, B. (1994) On neuronal specificity and the molecular basis of perception. *Cell*, **79**, 935–943.  
 Matsui, M. and Homma, H. (1994) Biochemistry and molecular biology of drug-metabolizing sulfotransferase. *Int. J. Biochem.*, **29**, 1237–1247.  
 Miyawaki, A., Matsushita, F., Ryo, Y. and Mikoshiba, K. (1994) Possible pheromone-carrier function of two lipocalin proteins in the vomeronasal organ. *EMBO J.*, **13**, 5835–5842.  
 Mulder, G.J. and Jakoby, W.B. (1990) Sulfation. In Mulder, J.G. (ed.), *Conjugation Reactions in Drug Metabolism*. Taylor and Francis, London, UK, pp. 107–161.  
 Pinching, A.J. and Powell, T.P.S. (1971) The neuropil of the glomeruli of the olfactory bulb. *J. Cell Sci.*, **9**, 347–377.  
 Ressler, K.J., Sullivan, S.L. and Buck, L.B. (1993) A zonal organization of odorant receptor gene expression in the olfactory epithelium. *Cell*, **73**, 597–609.  
 Ressler, K.J., Sullivan, S.L. and Buck, L.B. (1994) A molecular dissection of spatial patterning in the olfactory system. *Curr. Biol. Neurobiol.*, **4**, 588–596.  
 Vassar, R., Ngai, J. and Axel, R. (1993) Spatial segregation of odorant receptor expression in the mammalian olfactory epithelium. *Cell*, **74**, 309–318.  
 Weinshilboum, R. and Otterness, D. (1994) Sulfotransferase enzymes. *Handbook Exp. Pharmacol.*, **112**, 45–78.

Received on November 3, 1995; revised on December 19, 1995